Experimental Study on a Multi-evaporator Refrigeration System with Variable Area Ratio Ejector

Cui Li[a], Jia Yan[a, *], Yanzhong Li[a], Wenjian Cai[b] ,Chen Lin[b], Haoran Chen[b]

[a]School of Energy and Power Engineering, Xi'an Jiaotong University, Xi'an 710049, China

[b]EXQUISITUS, Centre for E-City, School of Electrical and Electronic Engineering, Nanyang Technological University, Singapore 639798

Highlights:

- Experiments are conducted on a multi-evaporator refrigeration system (MERS).
- The energy saved by ejector is up to about 12% compared to conventional PRV.
- Sufficient superheat is conducive to high performance and low power consumption.
- Ejector with variable area ratio is an effective response to varying cooling load.

Abstract: This paper describes an experimental study on a multi-evaporator refrigeration system (MERS) with conventional pressure regulating valve (PRV) and variable area ratio ejector. Some key performance indicators such as cooling capacity, power consumption and ejector entrainment ratio were evaluated by switching operating modes, adjusting superheat and tuning ejector spindle and so on. The results indicated that: 1) the energy efficiency of the MERS can be improved by up to 12% by replacing the conventional pressure regulating valve with the variable area ratio ejector, 2) sufficient superheat or superheat degree greater than 2℃ is conducive to high entrainment performance of the ejector, large cooling capacity of the low-temperature evaporator and low power consumption of the system, and 3) the effect of nozzle spindle position on the performance of the system is evident.

Keywords: Multi-evaporator refrigeration system; Variable area ratio ejector; Spindle; Cooling capacity allocation; Power consumption; Entrainment ratio

* Corresponding author: Tel.: +86 29 82668738; Fax: +86 29 82668725; Email: justinyan08@yahoo.com.

1. Introduction

The term of *refrigeration* can be defined as a process that removes heat to cool articles or substances down to, and maintain them at a temperature lower than the ambient temperature. It has many applications including but not limited to: air conditioning, household refrigerators and industrial freezers. In the present society, refrigeration has become one of the most energy-intensive sectors. Estimates are difficult to give but as an average for the developed countries, its share in electricity use is thought to be between 10-20% [1]. For tropical countries such as Singapore, this ratio can even rise to over 50% due to the hot and humid weather [2].

According to the evaporating temperature, refrigeration applications could be divided into three categories: high-temperature refrigeration, medium-temperature refrigeration and low-temperature refrigeration. Air conditioning is a good example of high-temperature refrigeration. Fresh food storage is in the medium-temperature range, while storage of frozen and dairy products is typical application of low-temperature refrigeration which generally starts at 0℃ to as low as -30℃[3]. In some circumstances, two or three evaporating temperatures can be involved. For example, in supermarket, approximately 50% of its total power consumption is associated with the medium and low temperature refrigeration [4-6], and 20% is used for air conditioning. Likewise, in applications such as food processing, transportation and storage, three evaporating temperatures, namely +7℃, –5℃ and –30℃, are usually required for space cooling, storage of perishable or temperature sensitive food, and freezing, etc. [7-9]. A convenient way to provide such cooling demands is to design a

complete refrigeration unit for each temperature range, but this is not economical because of the high total investment. An alternative to cope with applications involving two or more evaporating temperatures is to use multi-evaporators refrigeration system (MERS), a single refrigeration system which consists of one compressor, one condenser but two or three evaporators with each working at different evaporating temperature[10].

The conventional MERS uses pressure regulating valve (PRV) to maintain the required pressure differences between the high-temperature and low-temperature evaporators. Considering the pressure losses caused by the throttle effect of PRV, efficiency improvements of multi-evaporators refrigeration system may be achieved by replacement of pressure regulating valve. Several schemes have been proposed, for example, multistage refrigeration cycles [11, 12], cascade refrigeration cycles [11, 12], expander based MERS [13-15] and ejector based MERS. The first three schemes are often used in ultra-low temperature refrigeration (cryogenic refrigeration) or CO_2 refrigeration systems where the pressure and temperature of the refrigerant drop greatly after expansion process. However, for applications of MERS involving fresh storage, freezing and air-conditioning, the energy saving by such schemes are not significant. The last scheme uses ejector in place of PRV to recover the pressure loss associated with throttling, and this seems to be an appropriate energy-saving alternative. For example, L. Kairouani, et al. [16] recently proposed an energy-efficient three-evaporator refrigeration system with two ejectors. The results of exergy analysis show that the system COP can be improved by about 10% for

two-temperature ejector-based MERS and 20% for three-temperature ejector-based MERS, respectively, as compared to the conventional MERS.

The main drawback of ejector based MERS is that it can only work well at the on-design condition. This is difficult to guarantee in actual operation since the cooling capacity allocation between evaporators depends not only on the cooling requirements of target application but also on the ambient climate variations. Ejector with variable area ratio may go far towards solving the problem [17]. Li et al. [18] conducted an experimental study on the MERS with a variable area ratio ejector , and concluded that ejector should have an area ratio smaller than the critical value to guarantee its pressure recovery effect. However, to the best knowledge of the authors, no information is available with respect to the effects of refrigerant physical state, namely saturated or superheated state, on the ejector performance as well as the MERS.

In the present work, the conventional PRV and a variable area ratio ejector are used and compared in order to better respond to the varying cooling load, and to achieve an efficient running of the MERS at a wider range of conditions. The main target of this study is to obtain the optimal refrigerant states and ejector geometry so that the MERS is capable of meeting different cooling requirements with low power consumption. These findings are expected to contribute to the energy savings of the MERS, and can be easily extended to applications such as supermarkets, retail stores, shipping containers, food processing and service equipment, and chemical industries.

2. Experimental setup

The multi-evaporator refrigeration system (MERS) developed in the present study is schematically shown in Fig. 1. The main components of this test facility are: a BITZER 4cc-9.2 semi-hermetic type of inverter compressor, an air-cooled condenser, two electronic expansion valves (indicated by EEV1 and EEV2, respectively), two testing chambers, a variable area ratio ejector, and a pressure regulating valve (PRV). The well accepted refrigerant R134a is used as the working fluid. All the equipment and pipes in the present system are well insulated by foam rubber to prevent heat losses.

The two testing chambers are used to simulate the fresh food storage room with evaporating temperature of -5℃ and the freezing room with evaporating temperature of -30℃, respectively. Both chambers contain heat exchangers, blenders and power controllable heaters. The ethylene glycol solution is used for heat transfer with refrigerant, whose concentration is 20% (the corresponding freezing temperature is -8℃) for chamber 1 and 50% (the corresponding freezing temperature is -37℃) for chamber 2. The blender is driven by electrical motor and helps to increase the heat transfer rate in the testing chamber. The power controllable heater is applied so that the cooling load in the testing chamber can be adjusted according to the cooling demand. When the temperature reaches stable state in testing chamber, the cooling capacity is just the same with the heater power.

Since the two chambers work at different evaporating temperatures and pressures, two approaches are adopted to maintain the required pressure difference between the high-temperature and low-temperature evaporators. In other words, the system can

run in two modes, i.e., the conventional mode and the pressure recovery mode. In the conventional mode, the PRV is used and the refrigerant vapor at higher temperature is first throttled and then compressed by the compressor. In the pressure recovery mode, a variable area ratio ejector characterized by its adjustable area ratio takes the place of PRV. Besides keeping the required pressure difference, and the incentive for application of variable area ratio ejector also includes: (a) to get required allocation of cooling capacity by adjusting the entrainment rate of secondary fluid, and (b) to improve the system energy efficiency by the pressure recovery effect of the ejector and by the higher compressor efficiency resulting from the reduced compression ratio.

All the pressures are measured by pressure transducers with the accuracies of 0.5% of full scales. The temperatures are measured by PT1000 platinum resistance with an error of ±0.3℃. The flow rates are measured by two metal tube rotameters: one is mounted before EEV1 for refrigerant passing through the high-temperature evaporator, and the other is located before EEV2 for low-temperature evaporator. Each rotameter has an accuracy of ±1.6%.

The output signals from the measurement devices are transferred to a PC through a data acquisition board. The automatic monitor, control and data acquisition system is developed in Labview 2010 of the National Instruments [11], and can display the real-time working parameters and make record on demand. For a view of the real experimental rig and the monitor panel, see Fig. 2.

3. Geometric parameters of the variable area ratio ejector

An illustration of the variable area ratio ejector has been presented in Fig. 3. As

shown, it consists of five parts: the primary nozzle, the motor-driven spindle, the suction chamber, the mixing chamber, and the diffuser. The main geometry parameters of the ejector are designed according to refs. [19-21]. The constant-pressure section of mixing chamber has a converging angle of 25^{o}, while the constant-area section has a length (L) of 40 mm and a diameter (D) of 10mm. The primary nozzle used in the present study has an inlet diameter (d_1) of 15mm, throat diameter (d_2) of 4mm and exit diameter (d_3) of 6mm. It is placed upstream of the mixing chamber, and the distance between the exit of primary nozzle and the start of constant-area mixing chamber is 15mm. The motor-driven spindle is used for adjustment of primary nozzle. When the spindle moves, the effective flow area of nozzle throat changes, so does the ejector area ratio. The movement of spindle is described by the spindle position x, which is defined as the relative position of spindle tip in the primary nozzle. As illustrated in Fig. 3, x is negative when the spindle tip is in the convergent part of primary nozzle, equal to zero when the spindle tip moves to the throat section, and positive when the spindle tip is in the divergent part. And the relation between the spindle position x and the area ratio AR is as follows:

$$AR = \begin{cases} 6.25 & , \quad x \le 0 \\ \dfrac{5625}{900 - 4x^2} & , \quad 0 < x < 15 \end{cases} \tag{1}$$

The refrigerant coming from the high-temperature evaporator (Evaporator 1) enters the primary nozzle as the high-pressure primary fluid, while the refrigerant from the low-temperature evaporator (Evaporator 1) works as the entrained secondary

fluid. By moving the spindle inside the primary nozzle, it is possible to regulate the flow rates of primary and secondary fluids, which is an efficient adjustment in response to the variable cooling load .

4. Effect of working modes on the performance of MERS

As mentioned in Section 2, the multi-evaporator refrigeration system can run in two working modes, i.e., the conventional mode and the ejector-based pressure recovery mode. The two modes differ in the way of maintaining the required pressure difference between the high-temperature and low-temperature evaporators. The former uses a PRV to reduce the pressure of the high-pressure refrigerant stream before it mixes with the low-pressure stream, while the latter uses a variable area ratio ejector to accomplish both the decompression and mixing processes.

Since the two evaporators are used for different applications (Evaporator 1 for refrigeration and Evaporator 2 for freezing, respectively) and operate at different pressure and temperature levels, the power consumption rather than the coefficient of performance (COP) is used to evaluate the system performance. Specifically, the power consumed by the system is compared when each evaporator provides equal cooling capacity in both working modes.

A comparison experiment is carried out between the conventional mode and the pressure recovery mode. The results are shown in Fig. 4. It is found that power consumption increases linearly with the cooling capacity of Evaporator 1 in both conventional and pressure recovery modes. And the power consumption of conventional mode is higher than that of the ejector-based pressure recovery mode.

This means that the utilization of ejector helps to improve the energy saving effect of the whole system. The main reason is that refrigerant vapor at higher temperature suffers a pressure drop before it is compressed by the compressor, and compared with throttling of pressure regulating valve, ejector can recover part of the pressure loss associated with evaporating pressure difference. As a result, the compression ratio of compressor decreases while the compressor efficiency increases, which are beneficial to the reduction of power consumption.

It can also be concluded from Fig. 4 that the higher the cooling capacity of Evaporator 1 is, the more energy saving can be achieved by the ejector-based pressure recovery mode. For example, when the cooling capacity of Evaporator 1 is 1.0kW, the power consumption of pressure recovery mode is 1.95kW, saving about 2% in comparison with 1.99kW of the conventional mode. As the cooling capacity of Evaporator 1 increases to about 2.3kW, the power saved by the pressure recovery effect of ejector increases to about 12%. In other words, larger flow rate of high-temperature refrigerant stream makes the system more energy efficient. This is mainly because the pressure loss recovered by ejector is part of the pressure drop of the high-pressure refrigerant, and it increases with the increasing flow rate of high-pressure refrigerant since the pressure drop keeps constant at fixed evaporator pressures.

5. Effect of ejector primary fluid state on the performance of MERS

It is an important feature of the R134a T-S coordinate diagram that its specific entropy decreases with the rising temperature along the saturated vapor line. This

means that isentropic expansion of R134a from saturated vapor line will enter the wet–vapor region. As for ejector with R134a as working fluid, condensation may occur if the primary fluid is in or near the saturation state. This phenomenon could make quite an impact on the performances of ejector and MERS. In this section, superheat degree is considered as an indicator of primary flow physical state, and the dependencies of both system and ejector performances on superheat heat degree are analyzed in order to get a better understanding.

(1) System performance

The cooling capacity varies with the physical state of primary fluid. Take the operation condition listed in Table 1 as an example. The physical state of ejector primary flow changes from saturated state to superheated state when the ethylene glycol solution in the high-temperature evaporator is subjected to a sustainable temperature rise. In this process, the cooling capacities of both evaporators are strongly influenced. Fig. 5(a) shows a typical view of the cooling capacity variations with primary flow superheat degree, and the ejector geometry involved has a spindle position of -5mm and an area ratio of 6.25. The first and most obvious feature of these two cooling capacity curves is that the cooling capacity keeps almost constant as the superheat degree varies except close to the saturated point where drastic variation is observed. To be specific, the cooling capacity of the high-temperature evaporator (Evaporator 1) drops from 2.4kW to 1.9kW when the superheat degree increases from 0 to 2℃, and then keeps around 2.0 kW when superheat degree is further increased. Meanwhile, the cooling capacity of the low-temperature evaporator (Evaporator 2)

increases sharply from 0.7kW and then approaches a constant value of 1.1kW. Similar variations are observed for x=0, 5mm, 10mm (AR=6.25, 7.03, 11.25, respectively).

The power consumption of compressor varies in a way similar to the cooling capacity of Evaporator 1. That is, it first decreases rapidly and then keeps almost constant. This is in accordance with the linear relation of power consumption obtained in Section 3, and makes it possible to conclude that superheat is beneficial to energy saving.

(2) Ejector performance

The ejector performance is evaluated by the entrainment ratio which is defined as:

$$ER = \frac{m_s}{m_p} \tag{2}$$

where m_p is the mass flow rate of primary fluid, and m_s is the mass flow rate of secondary fluid. The entrainment ratio reflects to some extent the cooling capacity allocation between the two evaporators. The higher the entrainment ratio, the larger cooling capacity the low-temperature evaporator provides.

As shown in Fig 5(b), the entrainment ratio is strongly influenced by the superheat degree of primary flow. The entrainment ratio rises remarkably (from 0.25 to 0.55) when the superheat degree increases from 0 to 2℃ but little difference is observed when superheat degree is further increased. Similar variation of entrainment ratio to superheat degree are also founded for x=0, 5, 10 (see Fig 5(c)). It should be noted that the rapid increase of entrainment ratio is caused by the decreasing m_p and the increasing m_s. Therefore superheat is required to ensure high entrainment

performance and accordingly large cooling capacity of low-temperature evaporator. In other words, it is favorable to keep the primary flow under superheat condition from the viewpoint of exergy and energy quality.

Considering the different behavior of MERS and ejector, it is convenient to divide the primary flow states into two categories: the saturated state and the superheated state. The former one refers to the primary flow states close to the saturation curve and has a superheat degree less than 2℃. And the latter refers to the primary flow states with a certain degree of superheat, namely, the dry-vapor state. The temperature range of saturated state is a bit narrow comparing with the total error (about 0.6℃), which is calculated based on error propagation by taking into account not only the error of temperature sensor (0.3℃) but also the contribution of pressure sensor to error of saturated temperature (about 0.55℃ at 0.24MPa for pressure sensor with a range of 0~1.0MPa and an accuracy of 0.5%). However, the differences of system and ejector performances are fairly obvious between superheated and saturated conditions, and can be observed for different ejector configurations. At saturated primary state, variation of superheat degree causes rapid changes of cooling capacity, power consumption and entrainment ratio. While at superheated primary state, the effect of superheat degree is relatively small. This may be resulting from the fact whether the condensation process takes place in the primary nozzle. Since the saturated vapor line of R134a has a negative slope characteristic, the saturated primary fluid will enter the wet–vapor region when it expands inside the nozzle, and erosive droplets of high velocity appear accordingly. And the sensitivity of system performance to superheat

degree is considered to be a direct response to the generation of liquid droplets. On the other hand, if the inlet vapor of primary nozzle is superheated enough, the fluid remains in the dry–vapor state after expansion. In this case, the system performance appears to be independent of superheat degree.

6. Effect of ejector spindle position on the performance of MERS

As mentioned in section 3, the spindle in primary nozzle is movable under the driving of motor. When the spindle moves forward over the position $x = 0$, the effective flow area of nozzle throat will decrease, which leads to a rapid increase of area ratio.

The variation of ejector entrainment ratio with spindle position *x* is given in Fig. 6 and the corresponding test conditions are shown in Table 2. It can be seen that when the spindle position x varies between -5~0mm (*AR* maintains itself at a constant value of 6.25), entrainment ratios under both saturated and superheated conditions are almost kept unchanged. As the spindle moves forward further to 7.5 (the corresponding *AR* is 8.33), the entrainment ratio under superheated condition increases from 0.6 to 1.6 while the entrainment ratio under saturated condition increases from 0 to 0.75. This suggests that it is the area ratio of ejector rather than the spindle position that basically determines the variation of entrainment ratio. Furthermore, the entrainment ratio under superheated conditions is higher than that under saturated condition. In superheated conditions, therefore, the cooling capacity of low-temperature evaporator (Evaporator 2) makes up a larger portion when compared with the saturated condition. This is consistent with the results presented in

Section 5.

The effect of nozzle spindle position on the cooling capacity is depicted in Fig. 7 with (a) for high-temperature evaporator (Evaporator 1) and (b) for low-temperature evaporator (Evaporator 2). Still the cooling capacity keeps constant as the spindle moves in the primary nozzle until the area ratio of ejector begins to change. The cooling capacity of high-temperature evaporator (Evaporator 1) has a tendency qualitatively opposite to the entrainment ratio curve. It first keeps constant, say, 2.5kW for the saturated case, and then decreases with the spindle position. When the spindle tip moves to the position of 7.5mm (the corresponding *AR* is 8.33), the cooling capacity of high-temperature evaporator under saturated condition goes down to around 1.6kW. For the case of superheated primary state, this cooling capacity decreases gradually from 2kW to 1.25kW when the spindle position increases from a value of 0mm to 7.5mm. Unlike the high-temperature evaporator, the low-temperature evaporator (Evaporator 2) provides a cooling capacity proportional to the area ratio. When the spindle moves from 0mm to 7.5mm with the area ratio increasing from 6.25 to 8.33, the cooling capacity of Evaporator 2 increases from 0 to 1.25kW in saturated case and to 1.625kW in superheated case. Moreover, the cooling capacity of high-temperature evaporator under superheat condition is lower than that under saturated condition while the cooling capacity of low-temperature evaporator presents an opposite behavior.

Therefore, from a viewpoint of energy saving, large area ratio is recommended for high low-temperature cooling and low power consumption.

7. Conclusions

This paper is concerned with a multi-evaporator refrigeration system (MERS) that uses R134a as working fluid. The two evaporators of MERS are used for refrigeration and freezing, respectively. Efforts have been targeted at the feasibility of replacing the conventional PRV with a variable area ratio ejector to regulate their cooling capacity allocation and to recover the pressure loss. The primary findings can be summarized as follows:

(1) Energy efficiency improvements of MERS are achieved by replacing the conventional PRV with an ejector. In the range of cooling capacity measured in the present study, the energy saved by the pressure recovery effect of ejector is up to about 12%.

(2) The power consumption increases linearly with the cooling capacity of high-temperature evaporator (Evaporator 1) for both conventional and ejector-based pressure recovery working modes.

(3) Sufficient superheat or superheat degree greater than 2℃ is required to ensure high entrainment performance, large cooling capacity of low-temperature evaporator (Evaporator 2) and low power consumption.

(4) The cooling capacity of the system shows a strong dependence on the area ratio of ejector. When the spindle moves from 0mm to 7.5mm with the area ratio increasing from 6.25 to 8.33, the cooling capacity of Evaporator 2 increases from 0 to 1.25kW in saturated case and to 1.625kW in superheated case.

Acknowledgement

This work was supported by National Natural Science Foundation of China (Grant No. 51506158), the Fundamental Research Funds for the Central Universities and the A*STAR-MND Green Building Joint Grant of Singapore (1121760027).

Nomenclatures

d_1 inlet diameter of primary nozzle, mm

d_2 throat diameter of primary nozzle, mm

d_3 outlet diameter of primary nozzle, mm

D diameter of constant-area mixing chamber, mm

L length of constant-area mixing chamber, mm

m_P mass flow rate of primary flow, $kg \cdot s^{-1}$

m_S mass flow rate of secondary flow, $kg \cdot s^{-1}$

p_P primary flow pressure of ejector, bar

p_S secondary flow pressure of ejector, bar

p_b outlet pressure of ejector, bar

x the relative spindle position, mm

Abbreviation

AR ejector area ratio, $D^2 \cdot d_2^{-2}$

ER entrainment ratio, $m_S \cdot m_P^{-1}$

MERS multi-evaporator refrigeration system

PRV pressure regulating valve

Index

N1 inlet section of primary nozzle

N2 throat section of primary nozzle

N3 outlet section of primary nozzle

References

[1] L. Kuijpers. 2002 Report of the Refrigeration, Air Conditioning, and Heat Pumps Technical Options Committee. United Nations Environment Programme2003.

[2] B.K. Hodge, R.P. Taylor. Analysis and Design of Energy Systems 3ed. Prentice Hall1999.

[3] W.C. Whitman, W.M. Johnson, J.A. Tomczyk. Refrigeration & Air Conditioning Technology. 5 ed. Cengage Learning2005.

[4] J. Arias. Energy Usage in Supermarkets - Modelling and Field Measurements. Department of Energy Technology. Royal Institute of Technology, Stockholm, 2005.

[5] N. Rivers. Management of Energy Usage in a Supermarket Refrigeration System. THE INSTITUTE OF REFRIGERATION, London, 2005. p. 8.

[6] J.M. Garcia, L.M.R. Coelho. Energy efficiency strategies in refrigeration systems of large supermarkets International Journal of Energy and Environment 4(2010) 63-70.

[7] D. Datta, S.A. Tassou. Artificial neural network based electrical load prediction for food retail stores. Applied Thermal Engineering. 18 (1998) 1121-8.

[8] P.G. Jolly, C.P. Tso, Y.W. Wong, S.M. Ng. Simulation and measurement on the full-load performance of a refrigeration system in a shipping container. International Journal of Refrigeration. 23 (2000) 112-26.

[9] S.A. Tassou, J.S. Lewis, Y.T. Ge, H.I. Chaer. A review of emerging technologies for food refrigeration applications. Applied Thermal Engineering. 30 (2010) 263-76.

[10] W. Chen, X. Zhou, S. Deng. Development of control method and dynamic model for multi-evaporator air conditioners (MEAC). Energy Conversion and Management. 46 (2005) 451-65.

[11] S. Bhattacharyya, S. Bose, J. Sarkar. Exergy maximization of cascade refrigeration cycles and its numerical verification for a transcritical CO2–C3H8 system. International Journal of Refrigeration. 30 (2007) 624-32.

[12] M. Mafi, S.M.M. Naeynian, M. Amidpour. Exergy analysis of multistage cascade low temperature refrigeration systems used in olefin plants. International Journal of Refrigeration. 32 (2009) 279-94.

[13] B. Wang, H. Wu, J. Li, Z. Xing. Experimental investigation on the performance of NH3/CO2 cascade refrigeration system with twin-screw compressor. International Journal of Refrigeration. 32 (2009) 1358-65.

[14] J.A. Dopazo, J. Fernández-Seara. Experimental evaluation of a cascade refrigeration system prototype with CO2 and NH3 for freezing process applications. International Journal of Refrigeration. 34 (2011) 257-67.

[15] B. Zhang, X. Peng, Z. He, Z. Xing, P. Shu. Development of a double acting free piston expander for power recovery in transcritical CO2 cycle. Applied Thermal Engineering. 27 (2007) 1629-36.

[16] L. Kairouani, M. Elakhdar, E. Nehdi, N. Bouaziz. Use of ejectors in a multi-evaporator refrigeration system for performance enhancement. International Journal of Refrigeration. 32 (2009) 1173-85.

[17] C. Lin, W. Cai, Y. Li, J. Yan, Y. Hu, K. Giridharan. Numerical investigation of geometry parameters for pressure recovery of an adjustable ejector in multi-evaporator refrigeration system. Applied Thermal Engineering. 61 (2013) 649-56.
[18] C. Li, Y. Li, W. Cai, Y. Hu, H. Chen, J. Yan. Analysis on performance characteristics of ejector with variable area ratio for multi-evaporator refrigeration system based on experimental data. Applied Thermal Engineering. 68 (2014) 125-32.
[19] ASHRAE. Steam–jet refrigeration equipment. Equipment Handbook1979. pp. 13.1-.6.
[20] C. Li, Y. Li, L. Wang. Configuration dependence and optimization of the entrainment performance for gas–gas and gas–liquid ejectors. Applied Thermal Engineering. 48 (2012) 237-48.
[21] J. Yan, W.J. Cai. Area ratio effects to the performance of air-cooled ejector refrigeration cycle with R134a refrigerant. Energy Conversion and Management. 53 (2012) 240–6.

Figure captions

Fig. 1 Schematic view of the experimental rig

Fig. 2 Photograph of the experimental rig and user interface: (a) Experimental rig, (b) Monitor and control panel

Fig. 3 Schematic diagram and dimension of the variable area ratio ejector and primary nozzle

Fig. 4 Comparison of conventional working mode with pressure recovery mode

Fig. 5 Entrainment ratio and cooling capacity versus superheat degree: (a) cooling capacity ($x = -5$), (b) entrainment ratio ($x = -5$) and (c) entrainment ratio ($x = 0, 5, 10$)

Fig. 6 Variation of ejector entrainment ratio with spindle position at saturated and superheated conditions

Fig. 7 Variations of cooling capacity with spindle position at saturated and superheated conditions (a) cooling capacity of Evaporator 1, (b) cooling capacity of Evaporator 2

Figures

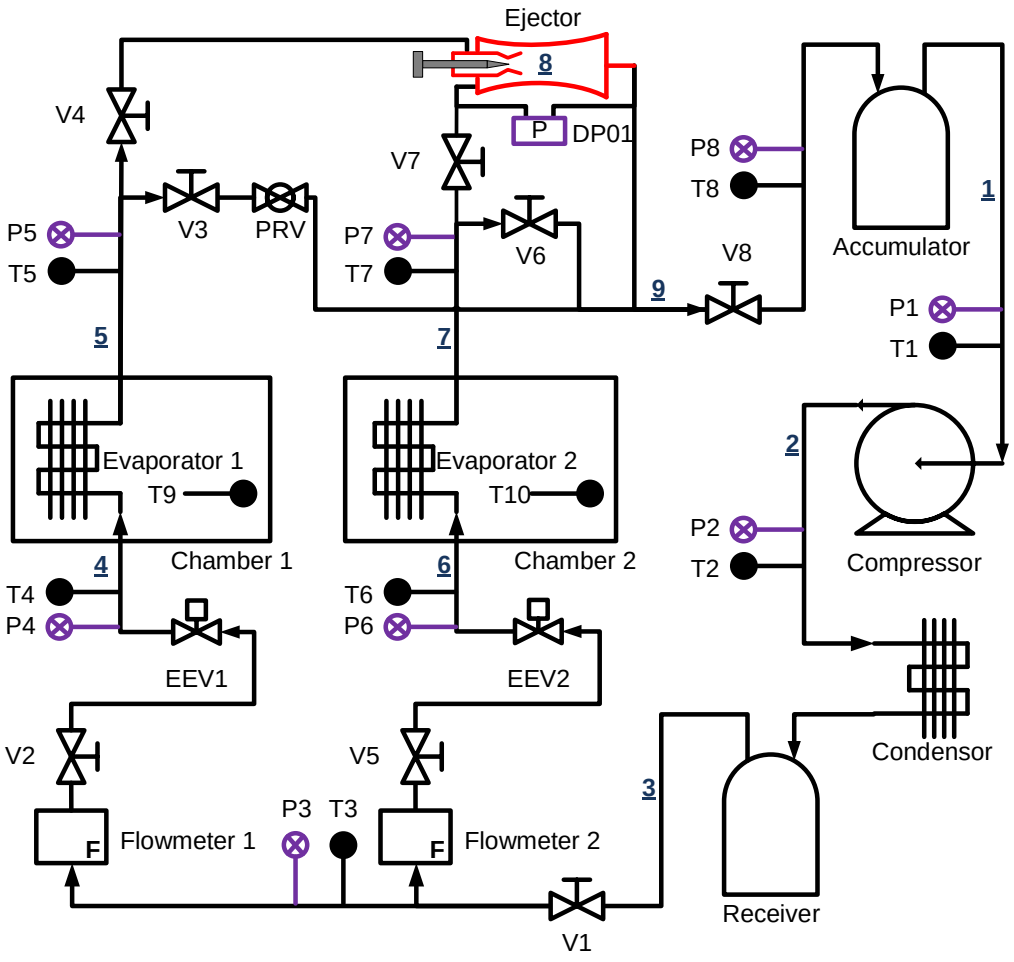

Fig. 1 Schematic view of the experimental rig

(a) Experimental rig

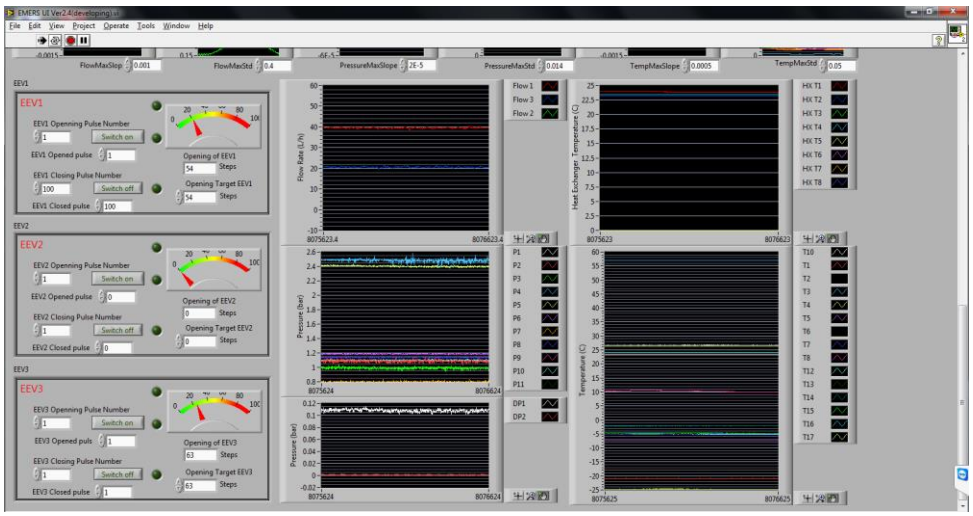

(b) Monitor and control panel

Fig. 2 Photograph of the experimental rig and user interface

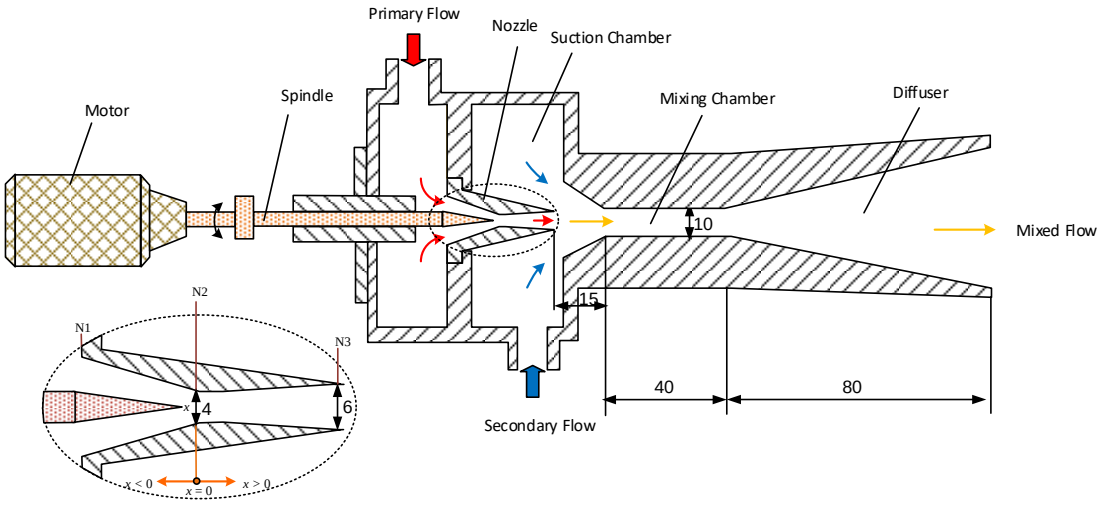

Fig. 3 Schematic diagram and dimension of the variable area ratio ejector

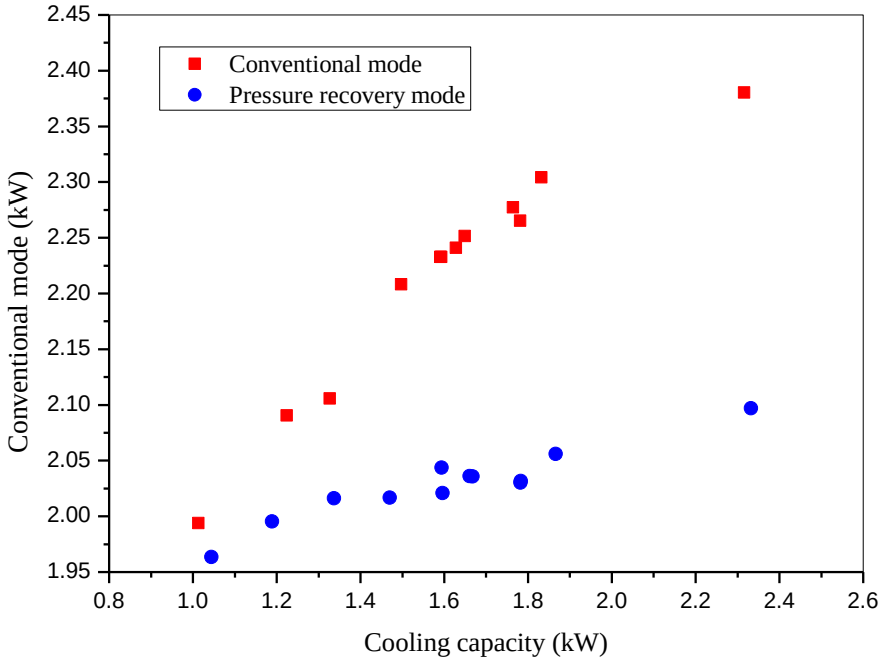

Fig. 4 Comparison of conventional working mode with pressure recovery mode

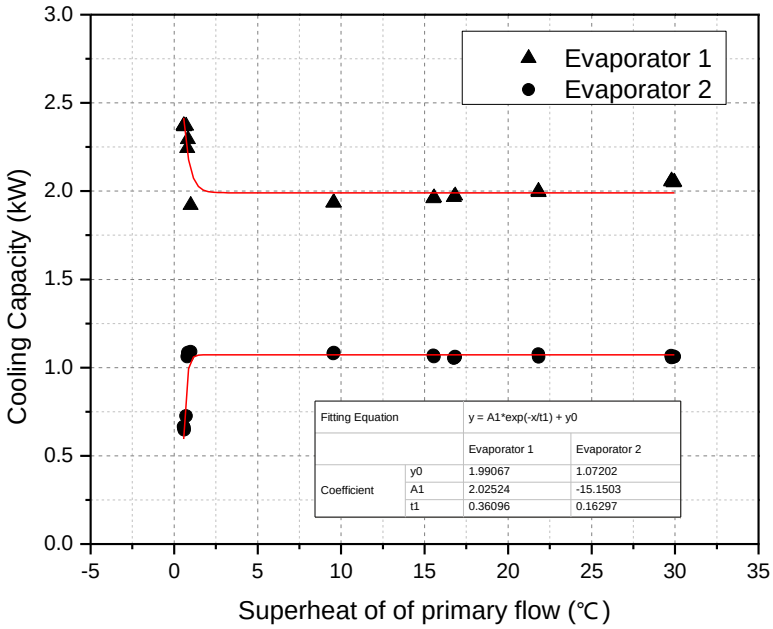

497

498 (a)

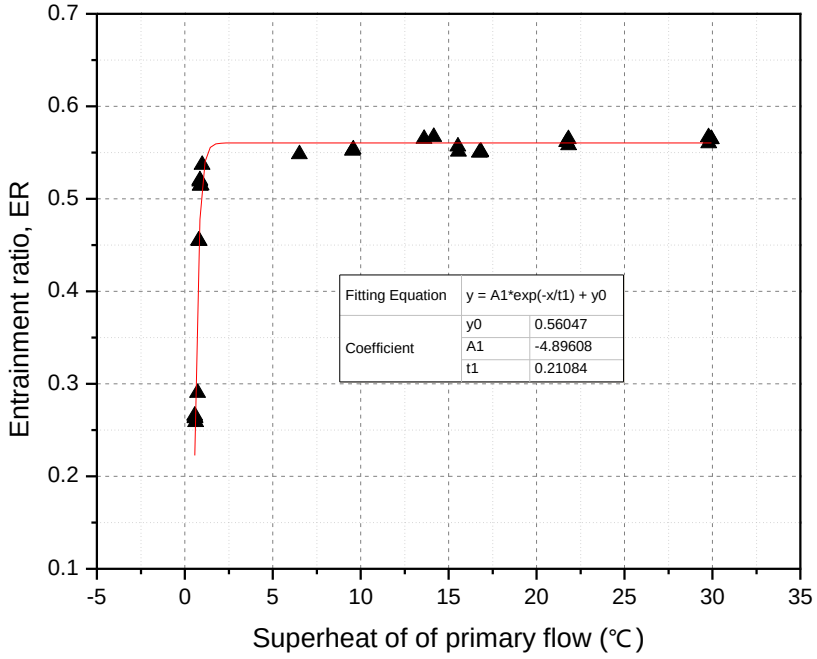

499

500 (b)

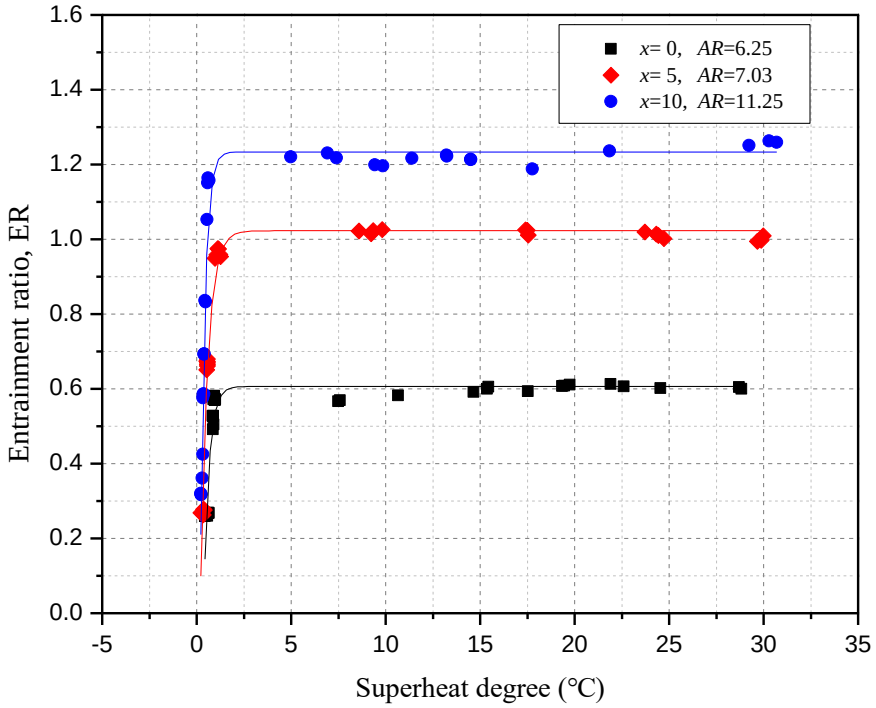

(c)

Fig. 5 Entrainment ratio and cooling capacity versus superheat degree: (a) cooling capacity ($x=-5$), (b) entrainment ratio ($x=-5$) and (c) entrainment ratio ($x=0, 5, 10$)

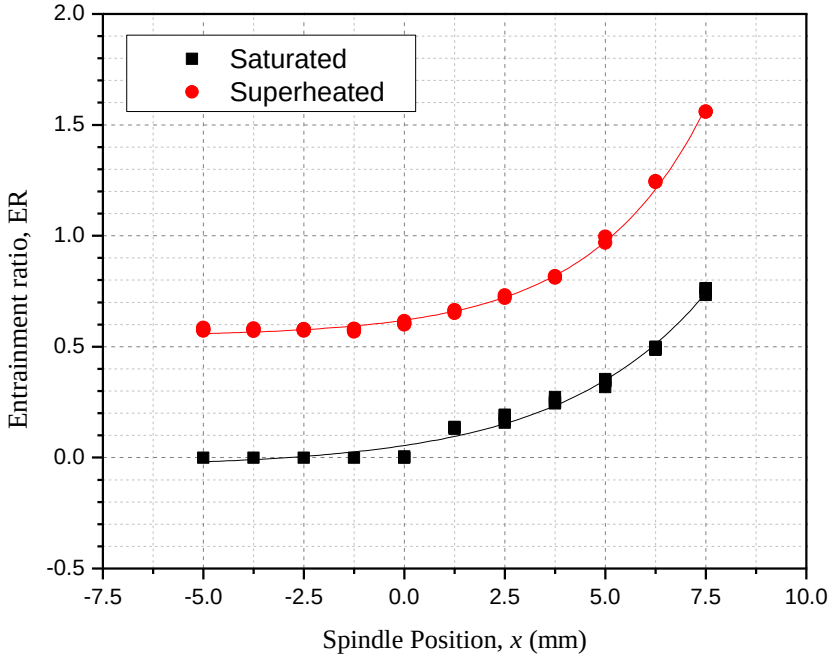

510

511

512 Fig. 6 Variation of ejector entrainment ratio with spindle position at saturated and superheated

513 conditions

514

515

516

517

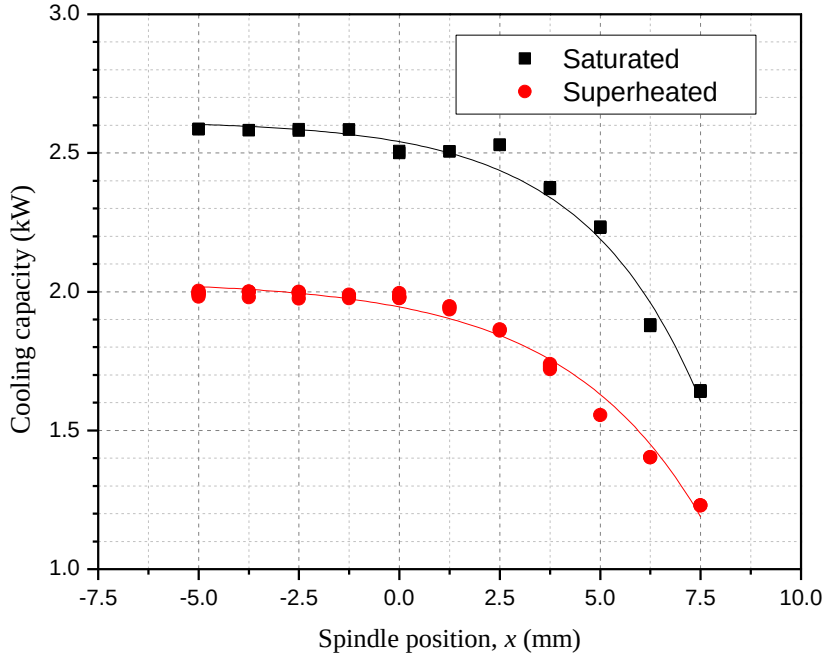

518

519 (a)

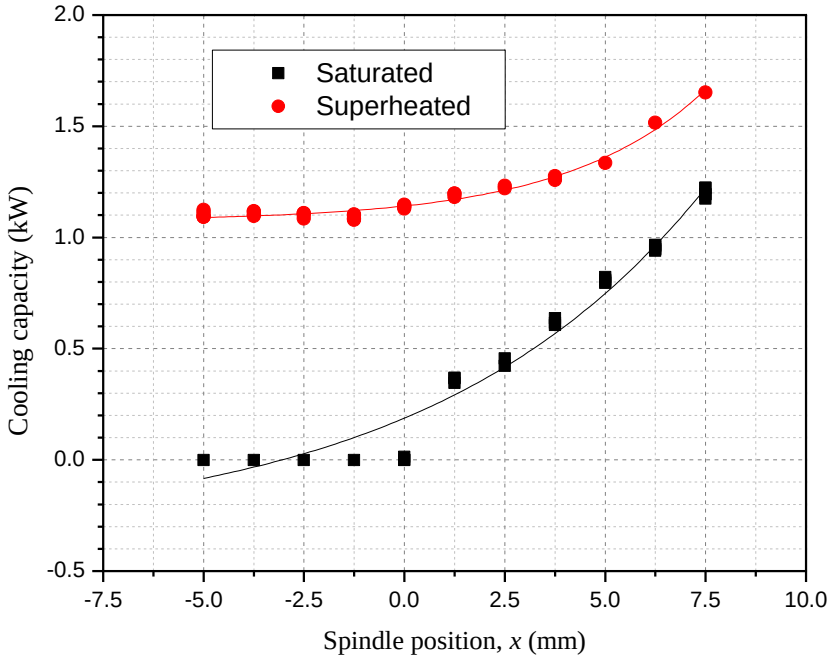

520

521 (b)

522 Fig. 7 Variations of cooling capacity with spindle position at saturated and superheated conditions

523 (a) cooling capacity of Evaporator 1, (b) cooling capacity of Evaporator 2

Tables

Table 1 Test conditions to study effect of primary fluid state

	Label	Application	Pressure (kPa)	Temperature of ethylene glycol solution (℃)
High-temperature evaporator	Evaporator 1	Refrigeration	240	5~25
Low-temperature evaporator	Evaporator 2	Freezing	110	-5

Table 2 Test conditions to study effect of ejector area ratio

Test Parameter	Label	Value
Primary pressure, p_P (kPa)	P5	240
Secondary pressure, p_S (kPa)	P7	110
Temperature of Evaporator 1 at saturated condition (℃)	T9	2
Temperature of Evaporator 1 at superheated condition (℃)	T9	15
Spindle position, d_{N1S1} (mm)		0 ~ 12.5
Area ratio		6.25~8.33